

Modelling and Simulation of Grid Connected Lithium-ion Battery Using HOMER

SHANTU GHOSE, ADEL EL-SHAHAT

Department of Electrical Engineering

Georgia Southern University

Statesboro, Georgia 30458

USA

sg04641, aahmed@georgiasouthern.edu

Abstract: - In order to improve battery technology understanding the capacity fading method in batteries is very important. Battery models can be used to predict their behavior under various operating conditions. Here we proposed a simple dynamic model of lithium-ion battery with MATLAB/Simulink to observe the output characteristics of this energy storage device. Dynamic simulations are carried out, including the observation of the changes in battery terminal output voltage under different discharging/charging, temperature and cycling conditions. The simulation studies are presented for proving that the model is useful. At the end we will use this energy storage device to interconnect with HOMER. Then different possibilities of producing electricity from various renewable energy sources like solar, wind etc. will be discussed by using HOMER. MATLAB software, Simulink, HOMER and Power System toolbox are used in modeling and simulation process..

Key-Words: - Simulink, SOC, dynamic mode HOMER, Li-ion battery.

1 Introduction

To make power networks more intelligent and encouraging with incorporation of renewable energy sources and storage devices are genuinely acknowledged as the essential initiative to accomplish a safe power sector [1] [2]. As fossil powers, for example, coal, oil are exhausting day by day, renewable energy sources have been urged to guarantee energy security of whole world. Most popular renewable energy sources like solar, hydro, biomass, biogas, wind and geothermal can give sensible imperativeness organizations. Within 2040, non-hydropower renewable vitality sources will represent more than 66% of the aggregate renewable era, while on the other hand, the aggregate renewable share of all power era will increment from 13% in 2013 to 18% in 2040 [3]. To store the energy we need backup system. For this reason, Li-ion batteries continue to be the reasonable choice for backup energy storage systems. It can be used for remote areas an optional and cleaner vitality source through the improvement of photovoltaic frameworks, hybrid electric vehicles and sun oriented power frameworks [4].

A battery can convert stored chemical energy into electrical energy with some internal heat losses [5]. Maximum capacity of a battery can be determined by SOC (state of charge), SOH (state of health) and SOF (state of function). SOC of a cell is the percentage of its total energy capacity that is still

available to discharge while on the other hand, SOH describes present condition and ability to deliver the specified performance compared with a new battery [6]. Li-ion batteries have greater power in a smaller package. It has fundamentally higher life cycle than lead acid battery in the field of discharge.

To understand the performance of Li-ion battery very well there are several models proposed by various authors [7-9]. Most of the models have many disadvantages where some of them did not include transient results [10] and some showed only SOC [11] or did not mention anything about battery runtime [12]. Numerical demonstrating could be utilized to defeat the restrictions in battery testing. Numerical displaying not just serves to enhance the comprehension of the battery working system yet, likewise gives inner data that are hard to acquire through investigations, for example, electrochemical response rates inside the cell, warm era, temperature dissemination, voltage dissemination, current dispersion, and so on. Different scientific models have been utilized to explore the warm reaction of the battery, for example, experimental conditions [13], electrochemical models [14-18], RC models [19-21], and lumped parameter models [22, 23].

Here we built up a successful dynamic lithium-ion battery recreation display in MATLAB/Simulink condition. The battery model is created tentatively through the [24], by including the huge temperature and limit blurring impacts on

battery flow. Dynamic simulations are utilized to confirm the execution of the created lithium-particle battery model, and the model is approved by contrasting and information acquired by a few reviews acknowledged by various creators.

2 Proposed Model

In this area, the dynamic model of the lithium-particle battery is presented. The model utilized as a part of [24] has been changed by including the impacts of temperature and limit blurring on battery yield attributes. The lithium-particle battery demonstrate parameters utilized as a part of proposed model are as per the following:

V_{bat} = Battery output voltage [V]

V_{oc} = Battery open-circuit voltage [V]

Z_{eq} = Battery equivalent internal impedance [Ω]

I_{bat} = Battery current [A]

$\Delta E(T)$ = Temperature correction of the potential [V]

SOC = State of charge

SOC_{init} = Initial state of charge

C_{usable} = Usable battery capacity [Ah]

T = Temperature [$^{\circ}C$ - $^{\circ}K$]

t = Storage time [months]

Q_n = Change in state of charge of battery negative electrode

N = Cycle number

k_1 = Coefficient for the change in SOC of battery negative electrode [$cycle^{-2}$]

k_2 = Coefficient for the change in SOC of battery negative electrode [$cycle^{-1}$]

k_3 = Coefficient for the change in R_{cycle} [$\Omega/cycle^{1/2}$]

CCF = Capacity correction factor

C_{init} = Initial battery capacity [Ah]

The battery yield voltage can be computed due to the battery open circuit voltage, voltage drop coming about because of the battery identical inner impedance and the temperature remedy of the battery potential. Likewise, the battery yield voltage might be communicated as [25]

$$V_{bat} = VOC - i_{bat} * Z_{eq} + \Delta E(T) \quad (1)$$

2.1 Open circuit voltage calculation

The battery open circuit voltage is the distinction of the electrical potential between the two terminals of a battery, at the point when there is no outside load associated. As the estimation of battery open circuit voltage is firmly reliant on battery SOC, it can be figured as

$$V_{oc}(SOC) = -1.031 \times \exp(-35 \times SOC) + 3.685 + 0.2156 \times SOC - 0.1178 \times SOC^2 + 0.321 \times SOC^3 \quad (2)$$

The battery SOC can be written as

$$SOC = SOC_{init} - \int (i_{bat} / C_{usable}) dt \quad (3)$$

2.2 Capacity fading

Capacity loss/ fading is a phenomenon observed in rechargeable battery usage where the amount of charge a battery can deliver at the rated voltage decreases with use. By and large, a battery is thought to be usable until coming to the 80% of its underlying limit [26, 27]. Side responses and debasement procedures may prompt various undesirable impacts, bringing about limit misfortune in lithium-particle batteries. Regularly, maturing happens because of numerous unpredictable marvels and responses that happen all the while at better places in the battery, and the corruption rate fluctuates between specific stages amid a heap cycle, contingent upon potential, neighborhood focus, temperature, and the heading of the current. Diverse cell materials age in an unexpected way, and the blend of various materials may bring about additionally quickened maturing due to, for example, "crosstalk" anode materials.

Demonstrating the limit blurring is imperative for foreseeing the remaining existence of the battery. The irreversible misfortune bringing about limit blurring is related with debasement of the battery, furthermore, the misfortune happens whether the battery is latent (alleged "calendar life" losses) or worked out ("cycle life" losses) [28]. Both calendar and cycle life losses of a battery seem, by all accounts, to be direct with time and significantly increment with expanding temperature [27]. Subsequently, the impact of temperature must be considered while demonstrating the limit blurring for a battery. The timetable and cycle life misfortunes prompt a limit amendment variable to decide the staying usable battery limit. The limit adjustment element can be figured as

$$CCF = 1 - (Calendar\ life\ losses + Cycle\ life\ losses) \quad (4)$$

Then the remaining usable battery capacity can be defined as

$$C_{usable} = C_{initial} \times CCF \quad (5)$$

Storage losses is occurred when the battery is inactive. Its equation can be written as

$$\% \text{ storage loss} = 1.544 \times 10^7 * \exp(40498 / (8.3143 * T)) * t \quad (6)$$

where T is the temperature in $^{\circ}K$.

It is a substantial supposition to consider that the main variable related with the other part of capacity

fading, cycle life losses, is the negative terminal SOC. The rate of progress in negative terminal SOC reliant on cycle number and temperature can be spoken to as [27]

$$d\theta_n/dN = k_1N + k_2 \quad (7)$$

where the coefficient k_1 represents limit misfortunes that increment quickly amid unfavorable conditions, for example, cycling at high temperature, and k_2 is an element to represent limit misfortunes under normal states of cycling. The estimations of the coefficients, k_1 and k_2 change contingent upon cycling temperature (Table 1). The varieties of negative anode SOC can be used for simulating the cycle life losses [27].

TABLE I VALUES OF TEMPERATURE DEPENDENT COEFFICIENTS

| Cycling temperature[°C] | k_1 [cycle ⁻²] | k_2 [cycle ⁻¹] | k_3 [Ω/cycle ^{1/2}] |
|-------------------------|------------------------------|------------------------------|---------------------------------|
| 25 | 8.5×10^{-8} | 2.5×10^{-4} | 1.5×10^{-3} |
| 50 | 1.6×10^{-6} | 2.9×10^{-4} | 1.7×10^{-3} |

2.3 Equivalent circuit of internal impedance of battery

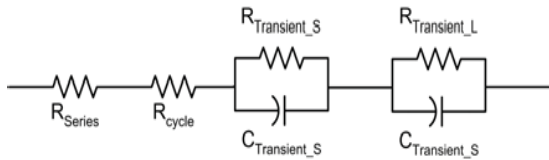


Fig. 1 Battery equivalent internal impedance

R_{series} is in charge of the prompt voltage drop in battery terminal voltage. The other part of arrangement resistor, R_{cycle} , is utilized to clarify the expansion in the battery resistance with cycling. The segments of RC systems are in charge of short and long-term homeless people in battery inside impedance. The estimations of R_{series} , $R_{Transient_S}$, $C_{Transient_S}$, $R_{Transient_L}$ and $C_{Transient_L}$ because of battery SOC can be computed as [29]

$$R_{series}(SOC) = 0.1562 \times \exp(-24.37 \times SOC) + 0.07446 \quad (8)$$

$$R_{Transient_S}(SOC) = 0.3208 \times \exp(-29.14 \times SOC) + 0.04669 \quad (9)$$

$$C_{Transient_S}(SOC) = 752.9 \times \exp(-13.51 \times SOC) + 703.6 \quad (10)$$

$$R_{Transient_L}(SOC) = 6.603 \times \exp(-155.2 \times SOC) + 0.04984 \quad (11)$$

$$C_{Transient_L}(SOC) = -6056 \times \exp(-27.12 \times SOC) + 4475 \quad (12)$$

And R_{cycle} can be expressed as [27]

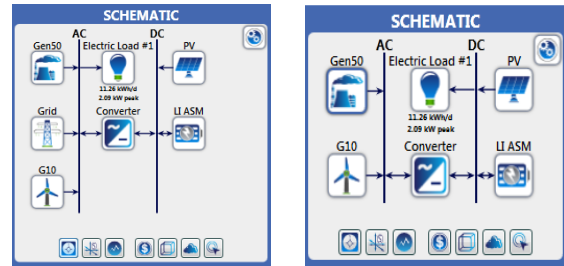
$$R_{cycle} = k_3 \times NI/2 \quad (13)$$

where the coefficient, k_3 independent of temperature changes which can be found from table

2.4 Temperature correction of the potential

$\Delta E(T)$ is a potential amendment term used to adjust for the variety of balance potential that is actuated by temperature changes. The figure portraying the change of $\Delta E(T)$ because of temperature can be found in Ref. [25].

3 HOMER Simulation Model



(a) (b)

Fig. 2 Structure plan in HOMER (a) on-grid (b) off-grid

From fig. 3 & 4 we can see that our proposed HOMER model consist of Generic 1kWh Li-ion/Lead-acid/Vanadium battery, PV cell, 10 kW wind turbine, 50 kW Genset generator, system converter and desired load. Here we considered residential load for all types of simulations. During normal operation hour load demand checked by PV cell and wind turbine however the additional energy from these parts is stored is put away in these batteries until full point of confinement of battery is come to.

HOMER simulation has two purposes. At the very beginning, it will check all feasibility of the system. HOMER considers the model to be workable in the event that it can sufficiently serve the electric load and fulfill some other requirements forced by the client. Secondly, the life-cycle cost of the system configuration is resolved, which is the aggregate cost of installing and operating the system over its life span. To evaluate the system performance under various operating conditions, simulation process have been carried out using HOMER built-in data (NASA Surface meteorology and Solar Energy) which is calculated based on location. During optimization, HOMER simulates various combination of the system and avoid the infeasible results. Then it shows the feasible results based on total net present cost (NPC). From these results we can choose the feasible output with

minimum net present cost. Optimization process decides the optimum value of every different results that interests the modeler [11].

For ideal cost estimation, HOMER simulates both off-grid and on-grid design under same load. Here, we used the following input parameters.

3.1 Generic flat plate PV

This photovoltaic array is flat plate type and manufactured by Generic.

3.2 Wind Turbine

In this paper, Generic 10 kW wind turbine is used.

3.3 Storage Devices

Here we used Generic 1kW Li-ion, Lead-acid & Generic Vanadium which is modified kinetic model battery. It includes rate dependent losses, temperature dependence on capacity, cycle lifetime estimation using Rainflow counting and temperature effect on calendar life. Additionally, it can support the system in off-grid mode.

3.4 System Converter

It is a system converter manufactured by Generic.

3.5 Advanced Grid

When there is insufficient power, the grid supplies power to meet the load demand. On the other hand, it consumes power when excessive power is available.

4 Simulation and Results

Based on the above equations we designed a lithium-ion battery model using MATLAB/Simulink

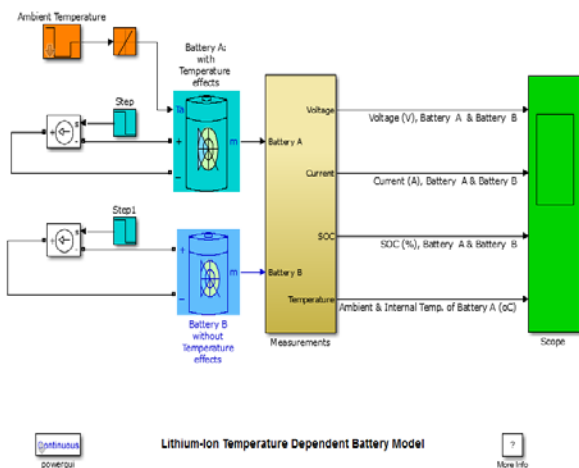


Fig. 3 Temperature dependent lithium-ion battery model

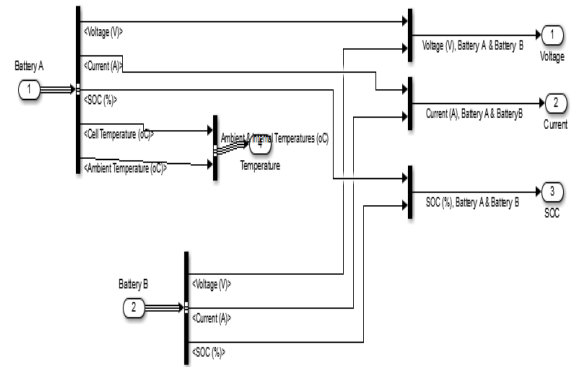


Fig. 4 Battery measurement circuit

This model outlines the impact of temperature on the execution of a 7.2 V, 5.4 Ah Lithium-Ion battery display. The model (which incorporates the effect of cell/encompassing temperature on the voltage, limit and resistance) is submitted to a variable surrounding temperature amid a release and charge handle. Its execution is contrasted with the situation where the effect of temperature is disregarded. As seen from the Scope, the temperature subordinate battery demonstrate performs near reality. As the cell/inward temperature expands/diminishes because of charge (or release) warm misfortunes and surrounding temperature varieties, the yield voltage and limit likewise increment/diminish.

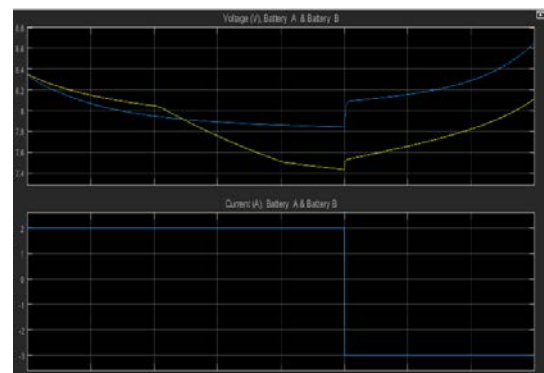


Fig. 5 Battery voltage and current

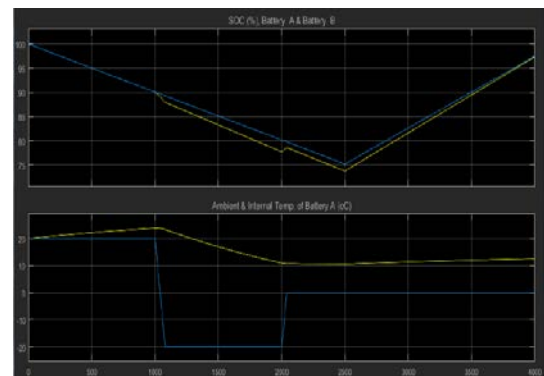


Fig. 6 SOC(%), Ambient & internal temp of battery A

The exhibit demonstrates the execution of the temperature subordinate Lithium-Ion battery display (Battery A) when the surrounding temperature is shifted from 20 degrees C to - 20 degrees C and afterward to 0 degrees C. Battery B speaks to the situation where the impact of temperature is disregarded. Begin the Simulation and open the Scope to view all signs.

At $t = 0$ s, the Battery A and B are released with 2A at surrounding temperature of 20 degrees C.

At $t = 150$ s, the inner temperature has expanded to its enduring state estimation of 29.2 degrees because of warmth misfortunes from the release procedure. This causes the yield voltage of Battery A to marginally increment, while battery B yield voltage keeps on diminishing.

At $t = 1000$ s, the surrounding temperature is diminished to - 20 degrees C. This causes the yield voltage of Battery A to significantly diminish as the inner temperature diminishes quickly. Additionally the SOC of Battery An abatements because of the decrease of battery limit. The battery B yield voltage keeps on diminishing gradually to its unflinching state voltage.

At $t = 2000$ s, the encompassing temperature is expanded from - 20 degrees C to 0 degrees C. As the inward temperature expands, the yield voltage of Battery An increments. Additionally, as the limit builds, the SOC of Battery An increments. The Battery B yield voltage stays consistent to its enduring state esteem.

At $t = 2500$ s, the Battery A and B are accused of 3 A at surrounding temperature of 0 degrees C. This makes the inside temperature increment because of warmth misfortunes amid the charge procedure, which builds the charging voltage of Battery A. A short time later, Battery A and B keep on charging up until completely charged.

After this battery model simulation we have used Li-ion for HOMER simulation. In this study, we have considered residential load. Assuming that, lifetime of whole project is 25 years. Fig. 6 and 7 shows the optimization results for our proposed model with and without grid connection respectively. Optimization process are carried out through every possible selection of variables in this hybrid power system without considering the sensitivity variables. According to fig. 8 total yearly production of our proposed model is 47,329 kWh/yr and consumption for residential load 43,391 kWh/yr.

The minimum COE obtained from the result is \$0.0618. In this scenario, the percentage of renewable energy contribution is 98%. In the

proposed grid connected model, an optimum number of renewable energy sources is activated and supplies electricity to the load. From Fig. 7, it can be clearly seen that off grid power system for the same load is more expensive (\$1.11) than grid connected system (\$0.0618). The NPC for on-grid and off-grid design is \$34,660 and \$58,714 respectively.

| Architecture | | | | | | | | | | Cost | | | System |
|--------------|--------------|-----------|------------|-------------|-----------|----------------|----------|----------|----------|---------------------|----------------------|----------------|--------|
| PV (kW) | PV-MPPT (kW) | Wind (kW) | Gen50 (kW) | LI-ASM (kW) | Grid (kW) | Converter (kW) | Dispatch | COE (\$) | NPC (\$) | Operating cost (\$) | Initial capital (\$) | Ren. Frac. (%) | |
| 250 | 250 | 1 | 100 | 20 | 999,999 | 28.0 | CC | \$0.0618 | \$34,660 | -\$1,246 | \$50,770 | 98 | |
| 250 | 250 | | 100 | 20 | 999,999 | 28.0 | CC | \$0.0770 | \$57,235 | -\$882.00 | \$48,770 | 95 | |

Fig. 7 Screenshot of optimized results (grid connected).

| Architecture | | | | | | | | | | Cost | | | System |
|--------------|--------------|-----------|------------|-------------|-----------|----------------|----------|----------|----------|---------------------|----------------------|----------------|--------|
| PV (kW) | PV-MPPT (kW) | Wind (kW) | Gen50 (kW) | LI-ASM (kW) | Grid (kW) | Converter (kW) | Dispatch | COE (\$) | NPC (\$) | Operating cost (\$) | Initial capital (\$) | Ren. Frac. (%) | |
| 250 | 250 | | 100 | 20 | 28.0 | CC | | \$1.06 | \$36,397 | \$388.96 | \$48,770 | 100 | |
| 250 | 250 | 1 | 100 | 20 | 28.0 | CC | | \$1.11 | \$58,714 | \$614.54 | \$50,770 | 100 | |

Fig. 8 Screenshot of simulation for finding optimal design (without grid).

5 Conclusion

In this paper, a dynamic model of lithium-particle battery considering the noteworthy temperature and limit blurring impacts is proposed. The recreation comes about demonstrates that the created model can genuinely mirror the dynamic yield normal for lithium-particle battery. The created model is ready to assess the battery execution under a few diverse working conditions, and it can be straightforwardly utilized as a part of diverse reproduction models including battery frameworks. On the other hand, for HOMER simulation we can conclude that grid connected hybrid power system which includes solar and wind is more cost effective than without grid connected for the same load. Our designed HOMER model with Li-ion battery is more cost efficient as our energy-cost-effective (COE) is 0.0618\$ kWh and the average residential electricity rate in Statesboro is 0.116\$ kWh [30].

References:

- [1] P. C. Loh, D. Li, Y. K. Chai and F. Blaabjerg, "Autonomous Operation of Hybrid Microgrid With AC and DC Subgrids," in *IEEE Transactions on Power Electronics*, vol. 28, no. 5, pp. 2214-2223, May 2013.
- [2] D. Boroyevich, I. Cvetkovic, R. Burgos and D. Dong, "Intergrid: A Future Electronic Energy Network?," in *IEEE Journal of Emerging and Selected Topics in Power Electronics*, vol. 1, no. 3, pp. 127-138, Sept. 2013.
- [3] "Annual Energy Outlook 2015," Report No. DOE/EIA-0383(2015), U.S. Department of

- Energy (DoE) / Energy Information Administration (EIA), Apr 2015.
- [4] T. Yamazaki, K. Sakurai and K. Muramoto, "Estimation of the residual capacity of sealed lead-acid batteries by neural network," *INTELEC - Twentieth International Telecommunications Energy Conference (Cat. No.98CH36263)*, San Francisco, CA, 1998, pp. 210-214.
- [5] Y. Xing, E. W. M. Ma, K. L. Tsui and M. Pecht, "Battery Management Systems in Electric and Hybrid Vehicles. *Energies*," 2011; 4, p.1840-1857.
- [6] W. Zhang, F. C. Lee and P. Y. Huang, "Energy management system control and experiment for future home," *2014 IEEE Energy Conversion Congress and Exposition (ECCE)*, Pittsburgh, PA, 2014, pp. 3317-3324.
- [7] K. A. Smith, "Electrochemical Modeling, Estimation and Control of Lithium-ion Batteries", Ph. D. Dissertation, Department of Mechanical Engineering, The Pennsylvania State University, USA, 2006.
- [8] D. W. Dees, V. Battaglia and A. Belanger, "Electrochemical modeling of lithium polymer batteries", *Journal of Power Sources* vol. 110, pp. 310-320, 2002.
- [9] P. Rong and M. Pedram, "Dynamic Lithium-Ion Battery Model for System Simulation", *IEEE Transactions on Very Large Scale Integration Systems*, vol. 14, pp. 441-451, 2006.
- [10] A. Hajizadeh and M. A. Golkar, "Intelligent power management strategy of hybrid distributed generation system", *Int. Journal of Electrical Power and Energy Systems*, vol. 24, pp. 783-795, 2007.
- [11] S. Buller, M. Thele, R. W. D. Doncker and E. Karden, "Impedance based simulation models of supercapacitors and Li-ion batteries for power electronic applications", *IEEE Transactions on Industry Applications*, vol. 41, pp. 742-747, 2005.
- [12] B. Y. Liaw, G. Nagasubramanian, R. G. Jungst and D. H. Doughty, "Modeling of lithium ion cells—A simple equivalent-circuit model approach", *Journal of Solid State Ionics*, vol. 175, pp. 835-839, 2004
- [13] Y. Chen, J.W. Evans, *J. Electrochem. Soc.* 141 (1994) 2947-2955
- [14] W.B. Gu, C.Y. Wang, B.Y. Liaw, *J. Power Sources* 75 (1998) 151-161
- [15] K.A. Smith, C.D. Rahn, C.Y. Wang, *Energy Convers. Manage.* 48 (2007) 2565-2578.
- [16] K. Smith, C.Y. Wang, *J. Power Sources* 160 (2006) 662-678.
- [17] G.H. Kim, A. Pesaran, R. Spotnitz, *J. Power Sources* 170 (2007) 476-489.
- [18] G.H. Kim, K. Smith, in: *214th Electrochemical Society Pacific Rim Meeting Honolulu, HI, 2008.*
- [19] A. Pesaran, *J. Power Sources* 110 (2002) 377-382.
- [20] M.W. Verbrugge, R.S. Conell, *J. Electrochem. Soc.* 149 (2002) A45-A53.
- [21] X. Hu, S. Li, H. Peng, *J. Power Sources* 198 (2012) 359-367.
- [22] P. Nelson, D. Dees, K. Amine, G. Henriksen, *J. Power Sources* 110 (2002) 349-356.
- [23] P. Nelson, I. Bloom, K. Amine, G. Henriksen, *J. Power Sources* 110 (2002) 437-444.
- [24] M. Chen and G. A. R. Mora, "Accurate electrical battery model capable of predicting runtime and I-V performance", *IEEE Transactions on Energy Conversion*, vol. 21, pp. 504-511, 2006.
- [25] L. Gao, S. Liu and R. A. Dougal, "Dynamic Lithium-Ion Battery Model for System Simulation", *IEEE Transactions on Components and Packaging Technologies*, vol. 25, pp. 495-505, 2002.
- [26] B. Kennedy, D. Patterson and S. Camilleri, "Use of lithium-ion batteries in electric vehicles", *Journal of Power Sources*, vol. 90, pp. 156-162, 2000.
- [27] P. Ramadass, B. Haran, R. White and B. N. Popov, "Mathematical modeling of the capacity fade of Li-ion cells", *Journal of Power Sources*, vol. 123, pp. 230-240, 2003.
- [28] R. Spotnitz, "Simulation of capacity fade in lithium-ion batteries", *Journal of Power Sources*, vol. 113, pp. 72-80, 2003.
- [29] M. Chen and G. A. R. Mora, "Accurate electrical battery model capable of predicting runtime and I-V performance", *IEEE Transactions on Energy Conversion*, vol. 21, pp. 504-511, 2006.
- [30] <http://www.electricitylocal.com/states/georgia/statesboro/>